RSC Advances

PAPER

View Article Online
View Journal | View Issue

Cite this: *RSC Adv.*, 2021, **11**, 33219

New insight into the joint significance of dietary jujube polysaccharides and 6-gingerol in antioxidant and antitumor activities

Zhen Wu, *[a] Ruiping Gao,[c] Hong Li,*[b] Yongde Wang,[a] Yang Luo,[a] Jiang Zou,[b] Bo Zhao[b] and Shiqi Chen[b]

Received 10th May 2021
Accepted 19th September 2021

DOI: 10.1039/d1ra03640h

rsc.li/rsc-advances

The combinatorial use of dietary jujube (*Ziziphus jujuba*) and ginger play a critical role in traditional Chinese medicines, folk medicine and dietary therapy. Joint effects were investigated from the viewpoint of the antioxidant (scavenging DPPH$^{\bullet}$) and antitumor activities (against SW620 cells) of jujube polysaccharides and ginger 6-gingerol (G6G) alone and in combination. Jujube polysaccharides were extracted, purified, and characterized, and then their inhibiting and apoptotic effects alone and in combination with G6G were evaluated by the cytological tests, including Cell Counting Kit-8, colony-forming, Annexin V-FITC and propidium iodide, TdT-mediated dUTP nick end labeling (TUNEL) staining, and cell cycle assays. Results showed that the purified polysaccharide fraction (ZJPs-II) with average molecular weight of 115 kDa consisted of arabinose, rhamnose, glucose, xylose, and galactose. ZJPs-II and G6G alone dose-dependently scavenged DPPH$^{\bullet}$ and inhibited the proliferation of SW620 cells, while their combination showed synergistic interactions (all combination index < 1). The studies further demonstrated that ZJPs-II and G6G alone reduced the cell colony-formation, induced apoptosis and arrested the cell-cycle at G2/M phase, while their combination achieved better effects and significantly arrested the growth at the G0/G1 phase. Collectively, our findings suggest enhancing the intake of jujube polysaccharides and G6G in a combinatorial approach for maintaining health and preventing cancer.

1. Introduction

Jujube (*Ziziphus jujuba*) and ginger (*Zingiber officinale*) together are very widely and frequently used in functional foods, herb tea and traditional Chinese medicine (TCM) prescriptions for centuries, especially in China. Nowadays, they have become more popular due to their unique taste, nutritional and functional properties.

Jujube is a famous culinary and medical fruit in Chinese daily diets for thousands of years. Among TCM, the dried jujube fruit was often used to invigorate the spleen, replenish *qi*, nourish the blood, and calm the nerves due to its therapeutic effects for anorexia, fatigue and loose stools in spleen deficiencies.[1] In recent years, modern pharmacological and nutritional studies have indicated that the jujube fruit could ameliorate hepatic function,[2] prevent neurodegenerative diseases,[3] improve memory,[4] and protect myocardia.[5] Those effects were mainly due to its richness in various nutrients, including polysaccharides, polyphenols, flavonoids, organic acids, vitamins, and microminerals.[6,7] As one of the most common components in the jujube fruit, polysaccharides might account for its crucial bioactivity.[8]

Ginger is known both as a TCM and popular food spice used globally, especially in China. Generally, it is popularly consumed as fresh ginger, dry ginger, and other ginger products to treat nausea, vomiting, digestive disorder, and diarrhea.[9] Recent research has found that ginger is rich in bioactive compounds, including gingerols, essential oils, and spicy substances. These compounds could exhibit various bioactivities, such as anti-hyperglycemic, anti-lipidemic, anti-inflammatory, alleviating the symptoms of gastrointestinal tract (GIT) illnesses and antioxidant functions.[10,11] Among them, the ginger 6-gingerol (G6G) was identified as the major component in either fresh or dried ginger, which exhibited several pharmacological and physiological activities.[12] More importantly, G6G was steadily distributed in GIT with the highest concentration among different blood and biological tissues after oral intake,[13] further exerting its activity on GIT and regulating the motility of GIT.[14]

It is known that the decoction and granule of the combination of jujube and ginger play a critical role in dietary and medical therapies. In the ancient Chinese book *Huangdi Neijing*

[a]*Chongqing Key Laboratory of Chinese Medicine & Health Science, Chongqing Academy of Chinese Materia Medica, Chongqing 400065, P. R. China. E-mail: wuzhen985@126.com; Fax: +86 23 81 38 16 17; Tel: +86 23 81 38 16 17*

[b]*Chongqing Institute for Food and Drug Control, Chongqing 401121, P. R. China. E-mail: hong198596@163.com*

[c]*College of Environment and Resources, Chongqing Technology and Business University, Chongqing, 400067, P. R. China*

(475–221 BC) and *Jin Gui Yao Lue* (25–220 AD), their combinatorial use was considered as the most frequently used herbal prescription.[15] The combined effects may be attributed to their involved polysaccharides, phenolic compounds and their interactions in nature.[16] As an example, Huang *et al.* found that combining jujube with green tea extracts exhibited the enhanced effects of anticancer activity in HepG2 cells.[17] This combinatorial effect was indirectly verified by many studies. Fang *et al.* found that a combination of *Coriolus versicolor* polysaccharides and flavonoid synergistically enhanced the learning and memory abilities for Alzheimer's disease.[18] Khawas *et al.* observed that *Piper nigrum* polysaccharide and piperine synergistically enhanced the antitussive effects.[19] Wang *et al.* reported that oolong tea polysaccharides, in combination with polyphenol, showed the synergistic effect on the mice tumor proliferation and growth *in vivo* due to their antioxidative and immune abilities.[20] Li *et al.* found that ginseng polysaccharides combined with ginsenoside Rb1 could enhance the hypoglycemic activity *via* regulating the intestinal flora.[21] You *et al.* reported that a combination of *Lycium barbarum* polysaccharides and grape seed procyanidins from complex extracts possessed the immune-enhancing function *in vivo*.[22] Chen *et al.* reported that pumpkin polysaccharides combined with puerarin ameliorated type II diabetes mellitus.[23] Additionally, naturally occurring polysaccharide–polyphenolic conjugates in herbal medicines played a key role on their bioactivities.[24] Therefore, natural polysaccharides in combination with phenolic compounds by physical or chemical approach are expected to improve the biological activities due to their cooperative therapeutic effects.[25,26]

Although the bioactivities of *Ziziphus jujuba* polysaccharides (ZJPs) and 6-gingerol alone have already been reported in the literature, their synergistic effects have not been probed.[27–29] To our knowledge, the joint effects and preliminary working mechanisms that underly the compatibility between ZJPs and gingerol have not been interpreted, which severely limits the efficient coadministration for enhancing their bioactivities. To uncover their joint significance, their combinative antioxidant and antitumor activities were probed with the purified ZJPs and G6G as representatives. Consequently, in the present study, after characterizing the physicochemical properties of the purified ZJPs, the antioxidant effect of the main ZJPs fraction and 6-gingerol alone and in combination was investigated *via* DPPH$^{\bullet}$, and their antitumor effects on human colon cancer SW620 cells were further evaluated *via* Cell Counting Kit-8 (CCK-8), colony formation, cell apoptosis, TdT-mediated dUTP nick end labeling (TUNEL) and cell cycle arrest assays. The results of this study will be useful to reveal their synergistic significance for functional complex applications in dietary and medical therapies.

2. Materials and methods

2.1. Materials

The dried jujube fruit (*Z. jujube cv. Ruoqiangzao*) was collected from Ruoqiang district (Xinjiang, China). Arabinose, rhamnose, glucose, xylose, galactose, galacturonic acid, trifluoroacetic acid, 1-phenyl-3-methyl-5-pyrazolone, D_2O, and DMSO were all purchased from Sigma-Aldrich (St. Louis, MO, USA). Ginger 6-gingerol (>98% purity) was purchased from Desite Biological Technology Co., Ltd. (Chengdu, China). DEAE-52 and Sephadex G-100 were obtained from Adamas Co., Ltd. (Shanghai, China). Dextrans (T-series 5-1100 k) and KBr (infrared spectroscopy grade) were bought from Aladdin Co., Ltd. (Shanghai, China). 1,1-Diphenyl-2-picrylhydrazyl (DPPH) was purchased from Xiya Reagent Co., Ltd. (Shandong, China). CCK-8, penicillin–streptomycin solution (100×), and trypsase (0.25%) were bought from Beyotime Co., Ltd. (Shanghai, China). L-15 medium, fetal bovine serum (FBS), and Dulbecco's modified Eagle's medium (DMEM) were bought from Gibco-BRL Co., Ltd. (NY, USA). Annexin V-fluoroisothio cyanate (FITC)/propidium iodide (PI) Apoptosis Detection Kit was obtained from YEASEN Biotech. Co., Ltd. (Shanghai, China). Cell Cycle Analysis Kit was purchased from Elabscience Biotech. Co., Ltd. (Wuhan, China). The TUNEL kit was purchased from Roche (Basel, Switzerland).

2.2. Extraction, separation, and purification of ZJPs

After removing seeds, the jujube fruit was pulverized into powders *via* a 40-mesh sieve for polysaccharide extraction. ZJPs was extracted by using an ultrasound-assisted method.[30] Briefly, the dried jujube powder was extracted with distilled water in an ultrasound bath at 83 °C and 140 W for 100 min. After filtering, the concentrated extract solutions were precipitated by 95% ethanol, 100% ethanol and acetone, respectively. The deproteinated solution *via* Sevag method was further dialyzed against distilled water for 2 days, and then lyophilized to obtain the crude ZJPs. To obtain the main fraction of ZJPs, the ZJPs dispersion was washed by DEAE-52 column (1.6 × 70 cm) with ultrapure water, followed by gradient sodium chloride solutions (0.1, 0.3 and 0.5 M) at a flowrate of 1 mL min^{-1}. The main ZJPs fraction was combined and concentrated, and finally purified by Sephadex G-100 column (1 × 100 cm). The elution fraction was detected by using the phenol–sulfuric acid assay at 490 nm. Finally, the main ZJPs fraction was collected, concentrated, dialyzed, and lyophilized.

2.3. Physicochemical characterizations of ZJPs-II fraction

The total carbohydrate content of the lyophilized ZJPs-II sample was measured by the phenol–sulfuric acid colorimetry assay using glucose as the standard.[31] The crude protein was quantified by Kjeldahl digestion using the conversion factor 6.25 (AOAC 955.04).[32] Uronic acid was assayed by *m*-hydroxydiphenyl method with galacturonic acid as the standard.[33] The ash was determined by muffle furnace (AOAC 942.05).[32] Moreover, its weight-average molecular weight (M_w) and monosaccharide compositions were measured by the previous method.[30] Briefly, the M_w was estimated by high performance gel permeation chromatography (E2695 with refractive index detector, Waters, USA). The test conditions were as follows: Shodex sugar KS-804 column, system temperature 35 °C, flow rate 1 mL min^{-1}, and injection volume 20 μL. The T-series dextrans (M_w 5k, 50k, 150k, 670k, and 1100k) were used as the standards to generate a calibration curve ($\log M_w = -0.3944T + 9.4412$, $R^2 = 0.9931$). For

assaying the monosaccharide compositions, the ZJPs-II samples were first hydrolyzed with trifluoroacetic acid, and then derivatized with 1-phenyl-3-methyl-5-pyrazolone. Afterward, the derivatives were determined by High Performance Liquid Chromatography (Shimadzu LC-2010A, Tokyo, Japan). The operating conditions were as follows: Kromasil C18 column, column temperature 30 °C, detecting wavelength 250 nm, flow rate 1 mL min^{-1}, and injection volume 20 μL. The eluent was composed of (A) 15% acetonitrile in 50 mM sodium phosphate (pH 6.9) and (B) 40% acetonitrile in 50 mM sodium phosphate (pH 6.9). The gradient profile was: 0–10 min, linear change from 0% to 10% eluent B; and 10–40 min, linear change from 10% to 30% eluent B.

To further reveal the typical compositions and functional groups of ZJPs-II, Fourier transform-infrared (FT-IR), ^{1}H and ^{13}C NMR measurements were performed. Briefly, ZJPS-II was mixed with KBr (1 : 100) and then measured using a Spectrum-100 spectrometer (PerkinElmer, USA) in the frequency interval of 4000–450 cm^{-1}. Prior to each NMR measurement, ZJPs-II was deuterium exchanged by continuously lyophilized operations. Then, the ZJPs-II D_2O-based solution (10 mg mL^{-1}) was measured using an Ultrashield 300 NMR spectrometer (Bruker, Germany) at room temperature.

To reveal the thermal properties of ZJPs-II, differential scanning calorimetry (DSC) was performed by DSC 4000 detector (PerkinElmer, USA). Briefly, the ZJPs-II sample (3.0 mg) was placed in an aluminium pan and heated from 25 to 400 °C at 10 °C min^{-1} in a nitrogen atmosphere (40 mL min^{-1}). Moreover, thermogravimetric (TG) and its first derivative (DTG) curves were obtained using a TGA 550 analyzer (TA Instruments, USA) in nitrogen atmosphere (40 mL min^{-1}) at temperatures ranging from 25 to 600 °C. The mass of the ZJPs-II sample was about 6.0 mg. The heating rate was 10 °C min^{-1}.

X-ray diffraction (XRD), scanning electron microscopy (SEM) and atomic force microscopy (AFM) were further used to investigate their molecular morphologies. Briefly, the lyophilized ZJPs-II sample was exposed to monochromatic Cu Kα radiation (40 kV and 30 mA) between the 2θ range of 5–70°. The diffractogram was obtained by using a D8-Advance diffraction system (Bruker, Germany). After vacuum coating with gold, the surface morphology of lyophilized ZJPs-II was examined by scanning electron microscope (Zeiss Supra-55, Germany). For AFM observation, ZJPs-II was first diluted with ultrapure water at a concentration of 2.5 μg mL^{-1}, and then about 2 μL of ZJPs-II solution was added to the mica surface and dried at room temperature. Subsequently, its surface morphology was observed by an AFM instrument (Bruker, USA) operated at tapping-mode. Finally, the obtained AFM results were analyzed with Gwyddion software (Brno, Czech Republic).

2.4. DPPH free radical (DPPH˙) scavenging capacities of ZJPs-II and G6G alone and in combination

According to our previous method,[34] 1 mL DPPH solution (0.1 mM in ethanol) and 3 mL aqueous solution of ZJPs-II (0–2.5 mg mL^{-1}), G6G (0–0.5 mg mL^{-1}), or their combination were mixed and shaken vigorously. After being put in the dark for 30 min, the absorbance of the mixture was measured at 517 nm. The DPPH˙ scavenging rate is calculated using eqn (1):

$$\text{Scavenging rate (\%)} = 100\% \times [A_0 - (A_1 - A_2)]/A_0 \quad (1)$$

where A_0, A_1, and A_2 represent the absorbances of the control (no sample), the sample, and the sample (no DPPH), respectively. The IC_{50} (50% inhibitory concentration) was obtained from the dose–effect curves.

2.5. Antitumor activities of ZJPs-II and G6G alone and in combination in SW620 cells

2.5.1. Cell culture conditions. The human colon cancer SW620 cells were purchased from the Chinese Academy of Sciences (Shanghai, China), and routinely maintained in DMEM with 10% FBS and penicillin–streptomycin antibiotic solutions at 37 °C (5% CO_2). ZJPs-II and G6G solutions were sterilized *via* 0.22 μm microfiltration prior to the antitumor test.

2.5.2. Inhibition rate assay. The CCK-8 assay was done to reveal the growth-inhibition effects of ZJPs-II and G6G alone and in combination on SW620 cells. Briefly, SW620 cells (1×10^5 cells per well) were seeded in 96-well plates at 37 °C for 12 h. Then, the cells were treated with a series of concentrations of ZJPs-II (25, 50, 100, 200, 400 and 800 μg mL^{-1}) and G6G (5, 10, 20, 40, 80 and 160 μg mL^{-1}) alone or in combination. After incubation for 24 h, 10 μL of CCK-8 solution was added to each well, and incubated at 37 °C for another 4 h. Finally, the absorbance at 450 nm was recorded by using a microplate reader (xMark, BioRad, USA). SW620 cells incubated in DMEM without any treatment served as a negative control. Each sample was tested three times. The growth-inhibition rate of the SW620 cells is calculated by the following formula:

$$\text{Inhibition rate (\%)} = 100\% \times [1 - (A_{\text{treat}}/A_{\text{control}})] \quad (2)$$

where A_{treat} and A_{control} are the absorbances of the treated and control cells, respectively. The IC_{50} value is obtained from the dose–effect curves.

2.5.3. Colony formation assay. The colony-forming assay was used to reveal the effects of ZJPs-II and G6G alone and in combination on the colonization potential of SW620 cells. Briefly, SW620 cells (1×10^5 cells per well) were seeded in the 6-well plates in growth media for 24 h, and then incubated with IC_{50} concentrations of ZJPs-II or G6G alone, or their combination for 10 days at 37 °C. The control cells were dealt with equal amounts of DMSO. After 10 days, the cell colonies were washed, fixed, and stained with crystal violet for 20 min. The excess dye was wiped off with phosphate buffered solution (PBS). Finally, the obtained colonies were photographed with an inverted fluorescence microscope (ECLIPSE Ti-s, Nikon, Japan) and analyzed.

2.5.4. *In vitro* cells apoptosis assay. Apoptosis was evaluated by staining SW620 cells with Annexin V-FITC and PI. Briefly, SW620 cells (1×10^5 cells per well) were plated in a 6-well plate and dealt with IC_{50} concentrations of ZJPs-II, G6G, and their combination for 24 h. The control cells were dealt with an equal amount of blank culture medium. After washing the

collected cells twice with PBS (pH 7.2), the cells were dyed with Annexin V-FITC and PI for 10 min in the dark (Rt). The treated and control cells were immediately measured by using CytoFLEX (Beckman Coulter, Inc. USA).

2.5.5. Morphological observation of SW620 cells. TUNEL staining was used to further detect apoptosis in SW620 cells treated with ZJPs-II, G6G, and their combination. The cell nuclei were stained with DAPI. Fluorescence images of SW620 cells were captured with confocal laser scanning microscopy (CLSM) (FV1200, Olympus, Tokyo, Japan).

2.5.6. Cell cycle assay. To measure the effects of ZJPs-II and G6G alone and in combination on the cell cycle distribution, SW620 cells were treated with the tested samples for 24 hours as indicated above. Afterward, the cells were trypsinized, harvested, and fixed with cold ethanol (70%) overnight at 4 °C. After washing with cold PBS, the cells were treated with RNase-A and PI at 37 °C for 30 min in the dark. The fluorescence intensity was immediately determined by flow cytometer (FACSVantage SE, BD Biosciences, USA).

2.6. Evaluation of the synergistic effects of ZJPs-II and G6G

Analysis of the synergism between ZJPs-II and G6G in scavenging DPPH˙ and inhibiting cell growth was done by the Chou–Talalay method reported by Chou.[35] The dose reduction index (DRI) and combination index (CI) values were obtained by using CompuSyn software (CompuSyn, Inc, USA). The DRI denotes the theoretical magnitude of the dose reduction that can be gained for each sample in combination compared to the dose of each sample alone that will generate a parallel efficacy. DRI > 1, DRI < 1 and DRI = 1 suggest favorable, unfavorable and no concentration–reduction effect, respectively. Moreover, CI = 1, CI > 1, and CI < 1 represent additive (or no interaction), antagonistic, and synergistic effects, respectively.

2.7. Statistical analysis

All data were presented as the mean ± standard deviation (n = 3). Statistical analyses were performed with SPSS v19.0 (IBM, Armonk, NY). The multiple comparison was performed by the least significant difference (LSD) test and differences with $p < 0.05$ considered as significant.

3. Results and discussion

3.1. Separation and purification of ZJPs

As depicted in Fig. 1a, one neutral polysaccharide and two acidic polysaccharides were identified by DEAE-52 cellulose column. The main ZJPs-II fraction was further verified by Sephadex G-150 column and only one single peak was detected (Fig. 1b), which indicated that ZJPs-II was homogeneous.

3.2. Structural analysis of ZJPs-II

The structural characterization of the polysaccharides is of great importance to reveal their structure–activities relationship because the differences of the chemical components, M_w and conformation of the polysaccharides will impact their structures and bioactivities. Therefore, the physicochemical characterizations of ZJPs-II are requisite. The total carbohydrate, uronic acid and ash amounts in ZJPs-II were 90.53 ± 5.22%, 5.31 ± 0.37% and 2.11 ± 0.12%, respectively. Notably, ZJPs-II did not contain protein. Moreover, ZJPs-II mainly consisted of arabinose, rhamnose, glucose, xylose, and galactose in a molar ratio of 26.31 : 8.62 : 18.35 : 15.72 : 5.52 (in molarity units, mmol L^{-1}). Its averaged M_w was determined as 115 kDa by high performance gel permeation chromatography. The main characteristic and functional groups of ZJPs-II was identified by FT-IR, as shown in Fig. 1c. Specifically, the broadly strong absorption band and slight absorption peak at about 3435 and 2931 cm^{-1} were caused by the O–H and C–H stretching vibrations, respectively. The two absorption bands were generally regarded as typical bands of polysaccharides.[36] The obvious absorption peaks at around 1744 and 1638 cm^{-1} were probably due to the C=O and COO^- stretching vibrations of the esterified groups, respectively, which indicated the presence of uronic acids.[37] The bands at 1405 and 1240 cm^{-1} belonged to the C–H bending vibration. The absorption band in the range of 800–1200 cm^{-1} was often considered as the "finger print" region of polysaccharides. The band in the range of 1000–1200 cm^{-1} suggested the stretching vibration of C–O–C and C–O–H. The weak peaks observed at 833 and 917 cm^{-1} was dominated by the α-glycosidic and β-glycosidic bonds of polysaccharides, respectively, which indicated that the α- and β-configurations co-existed in ZJPs-II.[38]

To further reveal the monosaccharide compositions, glycosidic linkages, and the detailed structural characteristics of ZJPs-II, ^1H and ^{13}C NMR spectra were obtained as shown in Fig. 1d and e, respectively. The signal around δ 4.70 ppm was due to solvent D_2O. Generally, the β-anomeric and α-anomeric protons mainly appeared in the δ 3–5 ppm and δ 5–6 ppm regions, respectively. The ^1H NMR spectrum of ZJPs-II displayed the anomeric signals in the range of 5.06–5.40 ppm due to the protons of the α-glycosidic bond, whereas the signals in the range of 3.16–4.94 ppm were attributed to the protons of the β-glycosidic bond, as well as the proton signals at C2–C6. This was consistent with the FT-IR spectrum. Based on the monosaccharide components and literature, the anomeric peaks located at δ 4.43, δ 4.63, δ 4.94, δ 5.12, and δ 5.22 ppm were attributed to the presence of β-D-Galp, β-D-Xylp, α-L-Rhap, α-D-Glcp, and α-L-Araf residues, respectively.[39–41] Additionally, the signal at approximately δ 2.05 ppm was assigned to the methyl proton and the obvious signals at δ 1.23 were assigned to the methyl proton of rhamnose.[42] The ^{13}C NMR signals in the range of δ 60–80 ppm were assigned to the carbon (C2, C3, C4, C5, and C6) on the other sites of the carbohydrate ring. The chemical shift at δ 181.16 ppm indicated the presence of uronic acid. The signal peak at 52.89 ppm indicated the existence of $-OCH_3$. Additionally, the signal at 100.42 was assigned to the branching units of β-Xylp.[43]

DSC was often used to reflect the thermostability and compatibility of polysaccharides and probe their intermolecular interactions. As presented in Fig. 1f, the DSC thermogram of ZJPs-II showed an endothermic band (crystallized temperature at 120.6 °C) and an exothermic band (256.8 °C). TG was further applied to describe the mass loss evolution of polysaccharides

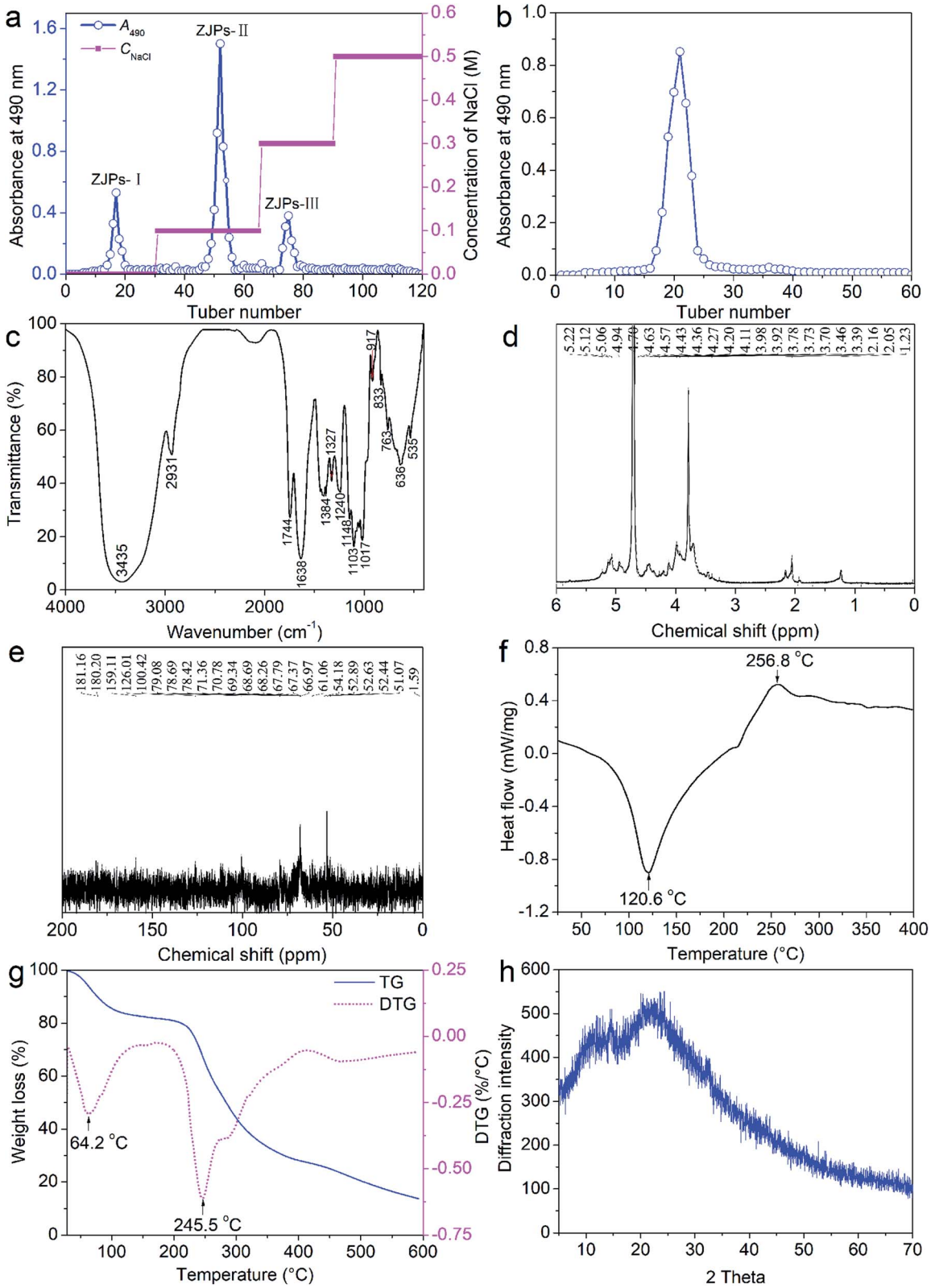

Fig. 1 Isolation and purification profiles of polysaccharides from *Ziziphus jujuba* fruits (ZJPs): (a) DEAE-52 cellulose column and (b) Sephadex G-100 column chromatography. Structural characterizations of the ZJPs-II fraction: (c) FT-IR spectrum; (d) ^{1}H NMR spectrum; (e) ^{13}C NMR spectrum; (f) differential scanning calorimetry (DSC) curve; (g) thermogravimetric (TG) and its first derivative (DTG) curves; (h) X-ray diffraction pattern.

under heating. Moreover, DTG could better differentiate their changing processes on the basis of TG. Two stages of TG/DTG curves were well identified in Fig. 1g. The first one covering from 25 °C to 150 °C was attributed to the loss of absorbed and structure water in ZJPs-II, and the mass reduced by nearly 15%. The second one ranging from 150 °C to 600 °C was due to the

oxidation of the carbonaceous residue formed during the decomposition of ZJPs-II, and the mass reduced by nearly 70%. The corresponding peaks in the DTG curve were located at 64.2 °C and 245.5 °C, respectively. The thermogravimetric events were in agreement with the DSC curve. These results indicated that ZJPs-II had potential as a functional material for food application because of its structural thermostability.

To probe the morphological features of the purified ZJPs-II fraction in detail, a combination of XRD, SEM and AFM techniques was directly used to investigate its crystalline state, surface, chain and corresponding aggregation conformation. XRD could reveal various features of polysaccharides, including the crystalline state, flexibility, swelling, and solubility.[44] Overall, a low crystallinity was confirmed from the XRD pattern of ZJPs-II shown in Fig. 1h. The main crystalline region was identified at around 12°, 20°, 24.3°, 25.5°, and 52.7° (2θ). However, other peaks were very weak and unresolved, or there were shoulders on more intense peaks.[45] The XRD analyses indicated that ZJPs-II was semi-crystalline polysaccharides. Similar polysaccharides with both crystalline and amorphous portions in their structures were extracted from other varieties of jujube.[45,46] The SEM results (Fig. 2a–c) showed that ZJPs-II had irregularly thin slice morphology with some thin debris and tiny bubble-like aggregates, which might be due to the combined effects of multiple molecular chains entanglement, ultrasonic cavitation and mechanical fluctuation.[47,48] Generally, the surface conformation of polysaccharides might be impacted by the extraction and preparation methods.[49] Moreover, the polysaccharides from different jujube varieties might have different monosaccharide compositions, M_w, chain arrangement and morphologies, which might be related to their bioactivities. The AFM images of ZJPs-II (2.5 μg mL^{-1}) are shown in Fig. 2d–f. In Fig. 2d and f, ZJPs-II showed equally distributed clusters with a large number of spherical aggregates and a small amount of dispersion. Their width ranged from 10 to 240 nm. However, the conformation revealed in AFM was different from that of SEM, which might be due to the freeze-dried state of the ZJPs-II material. The cross-sectional height profile in Fig. 2e indicated that the height of the spherical aggregates ranged from 1.2 to 3.4 nm. According to the previous result, the height range of the single chain for the polysaccharide molecule was 0.1–1 nm, which suggested that the polysaccharide chain of ZJPs-II might be interweaved and overlapped with each other and further formed spherical lumps.[8] Although ultrasound could disperse the polysaccharide clusters by destroying their noncovalent intra- and intermolecular interactions,[50] the dispersed polysaccharide molecules with many naked hydroxyl groups help form more intermolecular hydrogen-bonding interaction, resulting in a more complex microstructure of ZJPs-II.[30,47] Additionally, the structures of polysaccharides with specific particle size and surface charge might influence their functionalities and applications.[51]

As a kind of natural extract, ZJPs possess various properties, making it one of the favorable candidates for public health improvement and even cancer combination therapy.[52] After characterizing the purified ZJPs, the chief aim of the present work was to further explore the combinative effects of ZJPs-II and G6G in antioxidant and antitumor models *in vitro*.

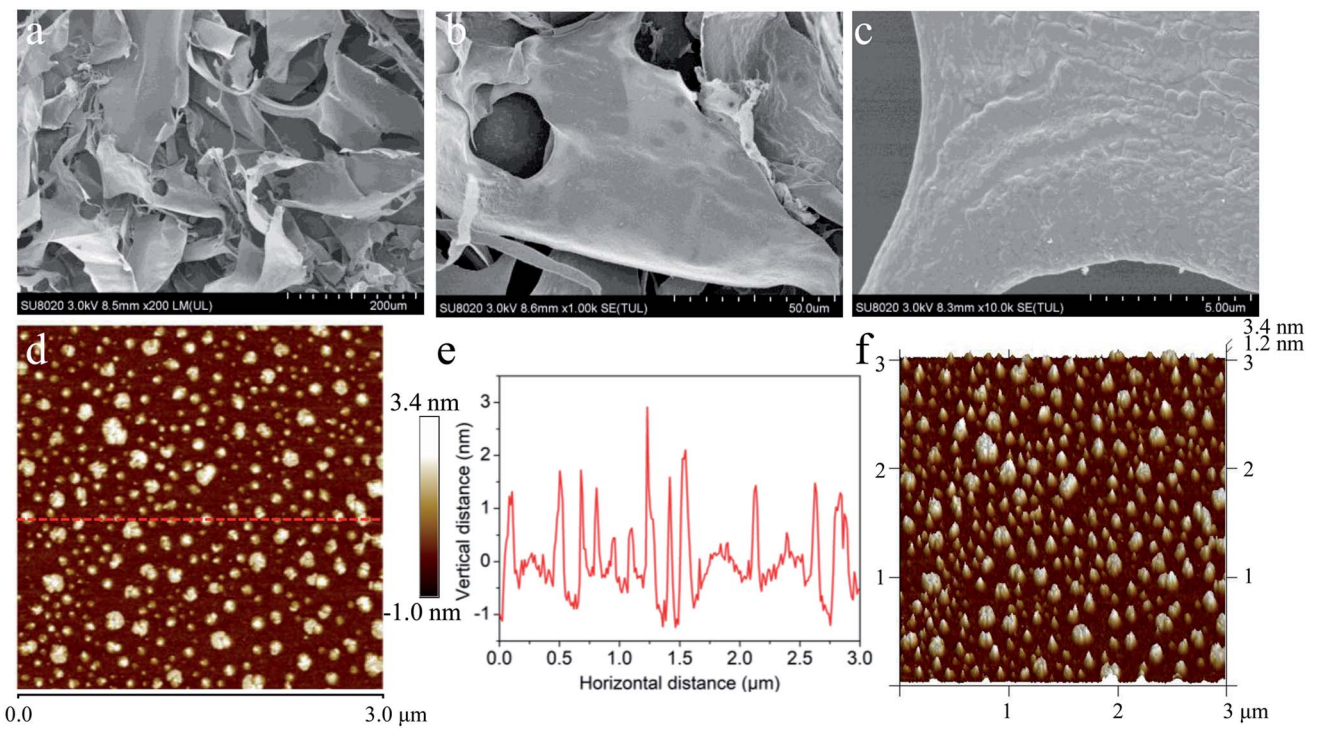

Fig. 2 Scanning electron microscopy ((a) ×200; (b) ×1000; (c) ×10 000) and atomic force microscope images ((d) the planar image; (e) the cross-sectional height profile; (f) three-dimensional image) of ZJPs-II (the dashed red line in (d) denotes the cross-section used for the determination of the height profile).

3.3. Antioxidant activity of ZJPs-II, G6G, and their combination *in vitro*

The oxidative stress results from an equilibrium among the oxidant–antioxidant courses: one causing the production of chemically reactive oxidants and the other detoxifying them or repairing the corresponding damage. Although these oxidants are generated mainly during normal cellular functions in our body, their excessive production may play a key role in the development of various chronic diseases, such as colorectal cancer.[53,54] Antioxidants, such as Z. *jujuba* polysaccharides and ginger phenols, can defend the human body against oxidative injury and further detoxify them.[8,10,11,52] In this section, we analyze in detail the DPPH• scavenging activity of ZJPs-II and G6G alone and in combination, which is a popular method for evaluating the antioxidant capacity of natural products *in vitro*. The result is shown in Fig. 3A. For all tested samples, the effects of scavenging DPPH• were in a dose-dependent manner. The IC_{50} values of ZJPs-II and G6G in eliminating DPPH• were calculated as 0.96 and 0.19 mg mL^{-1}, respectively. In comparison with ZJPs-II and G6G alone, this combination resulted in greater efficacy in scavenging DPPH•. Moreover, the DRI and CI values of their combination were calculated. As shown in Fig. 3B, the DRI values greater than 1 indicated favorable dose-reduction for the combination. The CI values less than 1 indicated that all of the tested doses had synergistic effects (Fig. 3C).

Nowadays, the antioxidant-based therapy is widely used in minimizing the complications related with oxidative stress in many diseases and even cancer. Many reports have demonstrated that antioxidant polysaccharides could prevent and/or ameliorate oxidative stress.[55,56] Bai *et al.* found that *auricularia auricular-judae* polysaccharides and grape seed procyanidins showed synergistic protective activities against radiation-damage *via* regulating the oxidative stress and antioxidative potential.[57] The antitumor activities of numerous phytochemicals were intimately associated with their antioxidant capacities,[58,59] which suggested that ZJPs-II and G6G together have promising activity for the prevention of cancer.

3.4. Antitumor effects of ZJPs-II, 6-gingerol and their combination *in vitro*

3.4.1. The cells growth-inhibition effects evidence. The anti-proliferative effects of ZJPs-II, G6G and their combination

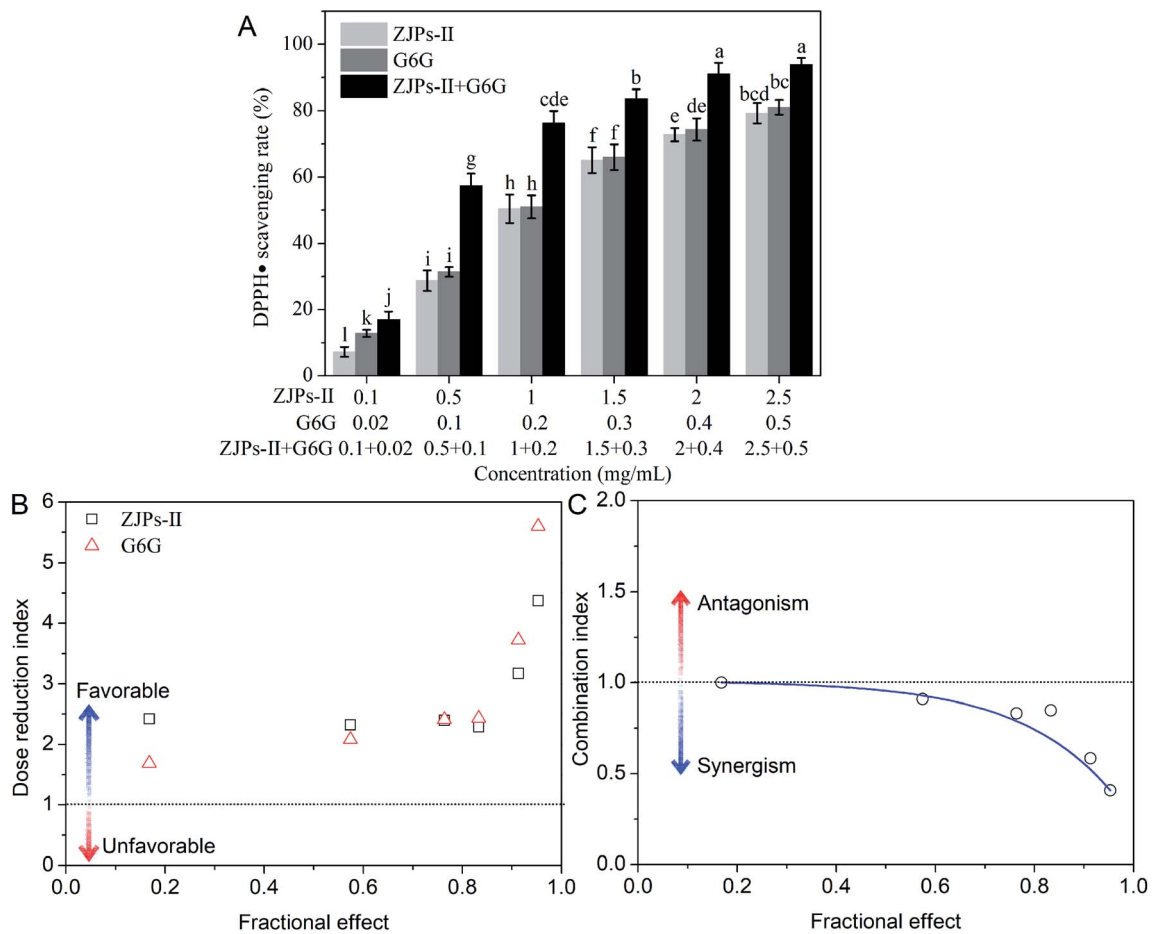

Fig. 3 Effects of ZJPs-II and ginger 6-gingerol (G6G) alone and in combination on scavenging DPPH• and corresponding synergistic result. (A) The scavenging rates of ZJPs-II, G6G and their combination on DPPH•. The number after each sample abbreviation represents its concentration (mg mL^{-1}). Different small letters (a–l) represent significant difference (LSD tests with $p < 0.05$). (B) The dose reduction index (DRI) and (C) combination index (CI) of the combination of ZJPs-II and G6G for scavenging DPPH• was calculated with CalcuSyn software.

on SW620 cells were estimated by CCK-8 assay, which is widely used to investigate the inhibitory activity of natural dietary compounds. Fig. 4A shows the concentration–effect curves of ZJPs-II, G6G and their combination. The growth of SW620 cells was significantly inhibited by ZJPs-II and G6G alone in a dose-dependent manner. At the highest concentrations of ZJPs-II (800 μg mL^{-1}), G6G (160 μg mL^{-1}), and their combination (800 + 160 μg mL^{-1}), the inhibitory rate was 54.0 ± 1.5%, 64.9 ± 1.3% and 75.5 ± 1.1%, respectively. More importantly, the inhibitory rate of the combination of ZJPs-II and G6G at each concentration was all significantly higher than that of the corresponding ZJPs-II or G6G alone ($p < 0.05$). Additionally, the IC_{50} values of ZJPs-II and G6G in inhibiting SW620 cell proliferation (in 24 h) were calculated as 752.3 and 66.0 μg mL^{-1}, respectively. Thus, the working IC_{50} concentration was chosen for subsequent experiments.

The nature of the interactions between ZJPs-II and G6G for inhibiting the growth of the SW620 cells was estimated by calculating DRI and CI according to the CCK-8 data, as shown in Fig. 4B and C. The DRI values for both ZJPs-II and G6G were above 1 for all combinations, which suggested favorable dose-reduction for each cotreatment. The CI values at a series of concentrations used ranged from 0.614 to 0.974, which indicated that the ZJPs-II and G6G combination had synergistic effects.

3.4.2. The colony formation evidence. The ability of the cells to maintain their clonogenicity after different treatments was assessed using the clonogenic assay. As shown in Fig. 5A, ZJPs-II and G6G alone significantly decreased the clonogenicity of the SW620 cells at its IC_{50} concentration by about 28.8% and 40.9% of the control ($p < 0.05$). This indicated that ZJPs-II and G6G alone could reduce the new colony formation and restrain the cell proliferation for a long period. More importantly, the combination of ZJPs-II and G6G reduced the colony formation by 58.8% of the control in SW620 cells, which indicated that the combination of ZJPs-II and G6G showed a more pronounced effect than either ZJPs-II or G6G treatment. The results were consistent with the inhibiting rates that we obtained from the CCK-8 test. Accordingly, we proved that their combination had significant inhibitory effects on the cell proliferation of SW620 cells compared to those of the individual treatment ($p < 0.05$). Additionally, the tumor cells invade almost exclusively in

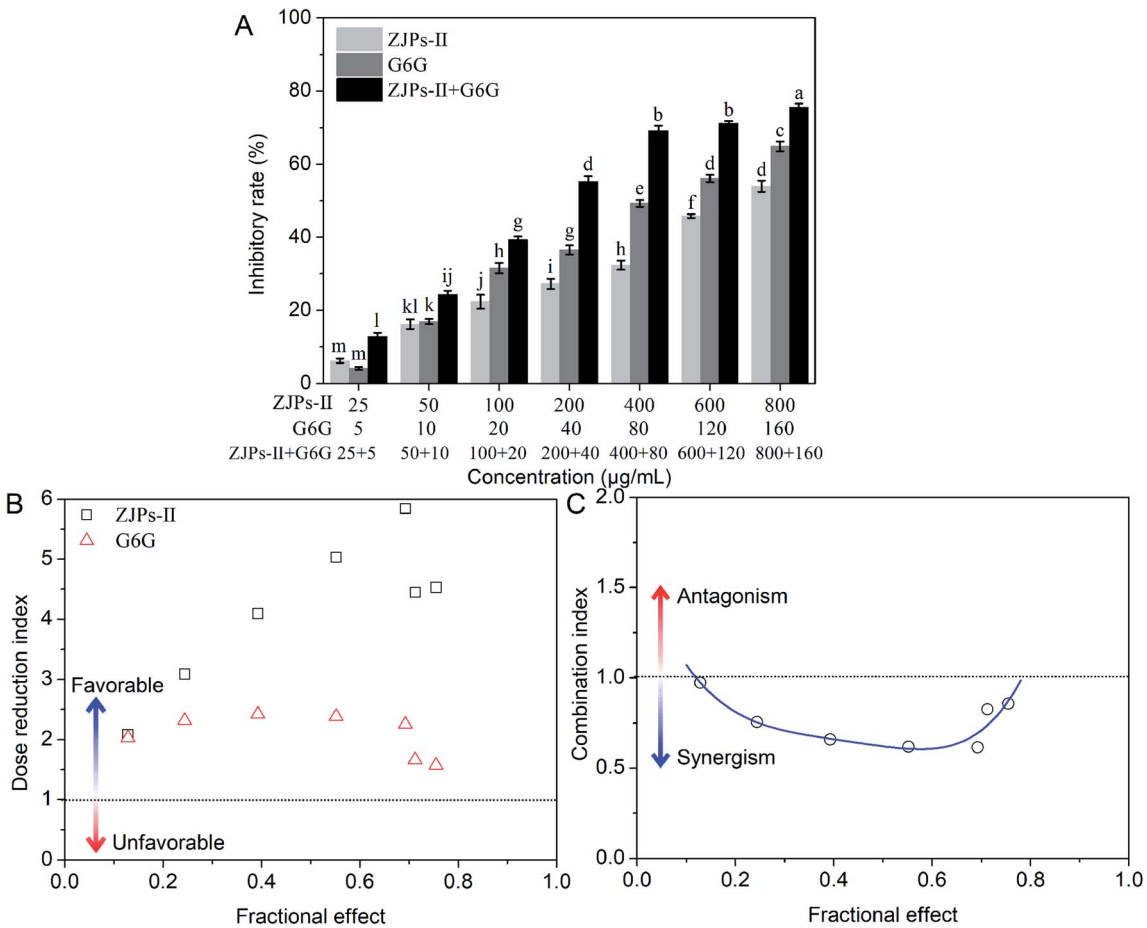

Fig. 4 Effects of ZJPs-II and ginger 6-gingerol (G6G) alone and in combination on inhibiting the growth of SW620 cells and corresponding synergistic result. (A) The inhibiting effects of ZJPs-II, G6G and their combination on the growth of the SW620 cells. The number after each sample abbreviation represents its concentration (μg mL^{-1}). Different small letters (a–m) represent a significant difference (LSD tests with $p < 0.05$). (B) The dose reduction index (DRI) and (C) combination index (CI) of the combination of ZJPs-II and G6G for inhibiting cell growth were calculated with CalcuSyn software.

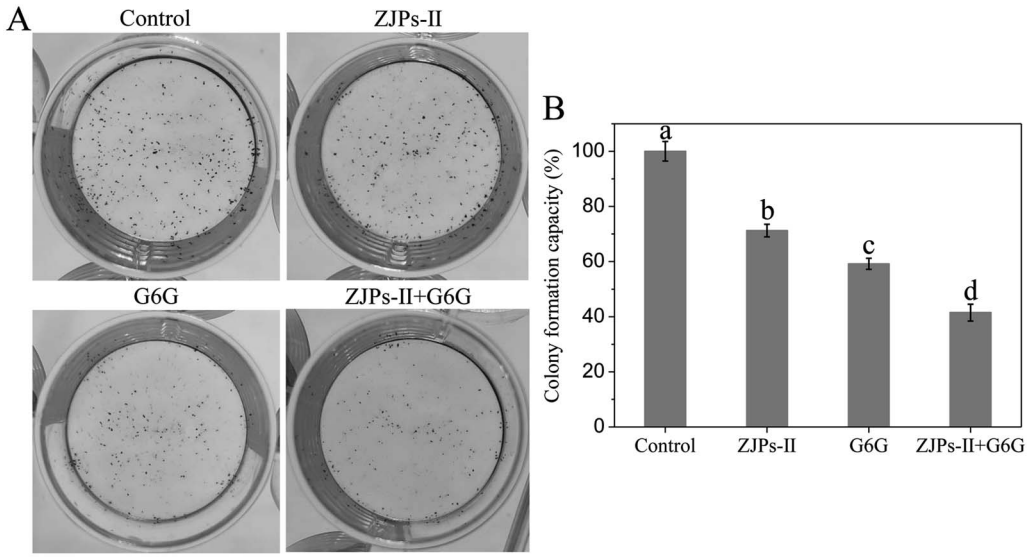

Fig. 5 Effects of ZJPs-II and ginger 6-gingerol (G6G) alone and in combination with IC_{50} concentrations on the colony formation of SW620 cells. (A) Representative images of colonies obtained after staining with crystal violet. (B) Bar graph represents the colony formation capacity for different treatments. The data were calculated from the average counting number of colonies per plate, as compared with the control (from three separate experiments). Different small letters (a–d) represent a significant difference (LSD tests with $p < 0.05$).

a collective way. Furthermore, they effectively colonize the secondary organs, which is mainly due to their invasiveness.[60,61] The findings also indicate that the combined use of ZJPs-II and G6G has an ability to weaken the invasiveness of the SW620 cells.

3.4.3. The cells apoptosis evidence. To clarify whether the inhibitory effects of ZJPs-II and G6G alone and in combination on the cell proliferation were related to apoptosis, SW620 cells were treated with IC_{50} concentrations of ZJPs-II and G6G, and their combination for 24 h, and the proportion of apoptotic cells was detected by flow cytometry. As shown in Fig. 6, the apoptotic proportions of the SW620 cells treated with ZJPs-II and G6G alone were 19.8 ± 1.2% and 18.5 ± 1.0%, respectively, while the apoptotic proportions of the SW620 cells treated with their combination was 60.2 ± 2.6%. Obviously, the apoptotic rate of the cells treated by the combination was 3 times higher than that of ZJPs-II and G6G alone.

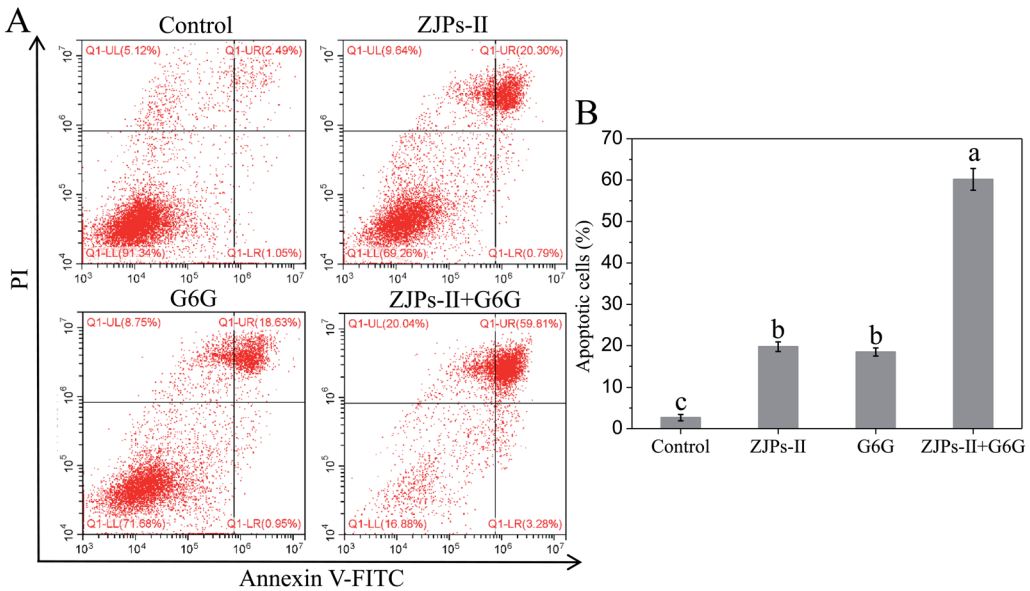

Fig. 6 Effects of ZJPs-II and ginger 6-gingerol (G6G) alone and in combination with IC_{50} concentrations on apoptosis in SW620 cells using flow cytometry. (A) Representative histograms of cells sorted by flow cytometry. Cells were treated with ZJPs-II and ginger 6-gingerol (G6G) alone and in combination, and stained with FITC labeled-Annexin V and propidium iodide (PI) before being sorted using flow cytometry. Cells in quadrants Q1, Q2, Q3, and Q4 denote necrotic, late apoptotic, viable (live), and early apoptotic populations, respectively. (B) Quantification of apoptotic cells. Data are expressed as the mean ± SD ($n = 3$). Different small letters (a–c) represent significant difference (LSD tests with $p < 0.05$).

To directly observe the apoptotic cell death in SW620 cells under the control and treated with ZJPs-II and G6G alone and in combination, we used the TUNEL assay to detect DNA fragmentation and cell death. The control and treated SW620 cells were observed with CLSM, and their representative images are shown in Fig. 7. The nuclei of the control SW620 cells were large and round without shrinkage, condensation and DNA fragmentation. However, in comparison with the control, all treated SW620 cells presented some common apoptotic features, including chromatin condensation, apoptosis bodies and fragmentation. SW620 cells treated with ZJPs-II and G6G alone showed similar apoptosis effects. Moreover, compared with the cells treated with ZJPs-II and G6G alone, SW620 cells treated with ZJPs-II and G6G in combination presented the largest variations in their morphologies and the lowest number of living cells. The results suggested that ZJPs-II and G6G might inhibit the proliferation of SW620 *via* synergistically inducing the apoptosis effect.

In general, a high antitumor ability may be relevant to the induction of apoptosis, necrosis, and/or intermediate phenotypes (aponecrosis) of cancer cells that are the classical phenotypes of programmed cell death with different morphologies.[62,63] Among them, apoptosis could be further induced into different cell forms by various natural extracts, and their morphological changes were due to the intensities of stimuli and their interactions. Furthermore, it is now commonly accepted that both apoptosis of cells and its sensitivity to diverse apoptotic stimuli are a series of direct gene-regulated processes,[62] but this requires further research.

3.4.4. The cell cycle arrest evidence. To further understand the preliminary working mechanism underlying the inhibitory effect of ZJPs-II and G6G alone and in combination against SW620 cells growth, we performed the cell cycle stages with flow cytometry. The distributions of treated and control cells in different cell cycle phases are shown in Fig. 8A. The percentages of cells in the G0/G1 phases treated by ZJPs-II and G6G alone were not significantly different compared to the control cells (Fig. 8B). Subsequently, the percentages of cells in the S phase were significantly decreased, while those in the G2/M phases were significantly increased compared to the control cells, which indicated that the cell cycle was slightly arrested at the G2/M phases by ZJPs-II and G6G alone. When they were used in combination, the population of SW620 cells in the G0/G1 phases (62.0 ± 2.9%) was significantly increased compared with the control ones (50.0 ± 1.0%). By contrast, the S phase and G2/M phase populations of SW620 cells treated by the combination were significantly reduced to 27.1 ± 2.0% and 10.9 ± 1.8%, respectively, compared with those of the control cells (34.8 ± 1.4% and 15.2 ± 0.5% respectively). These results evidently proved that ZJPs-II and G6G used in combination potentially arrested the cell cycle of the SW620 cells in the G0/G1 phases. This was different from the arresting mechanism of ZJPs-II and G6G alone. An understanding of the cell cycle distributions of SW620 cells treated by ZJPs-II and G6G alone and in combination might offer critical insight into regulating the cell cycle. Therefore, we revealed the possible role and preliminary action mechanism of the cell cycle arrest in the growth-inhibition of SW620 cells induced by the combination of ZJPs-II and G6G.

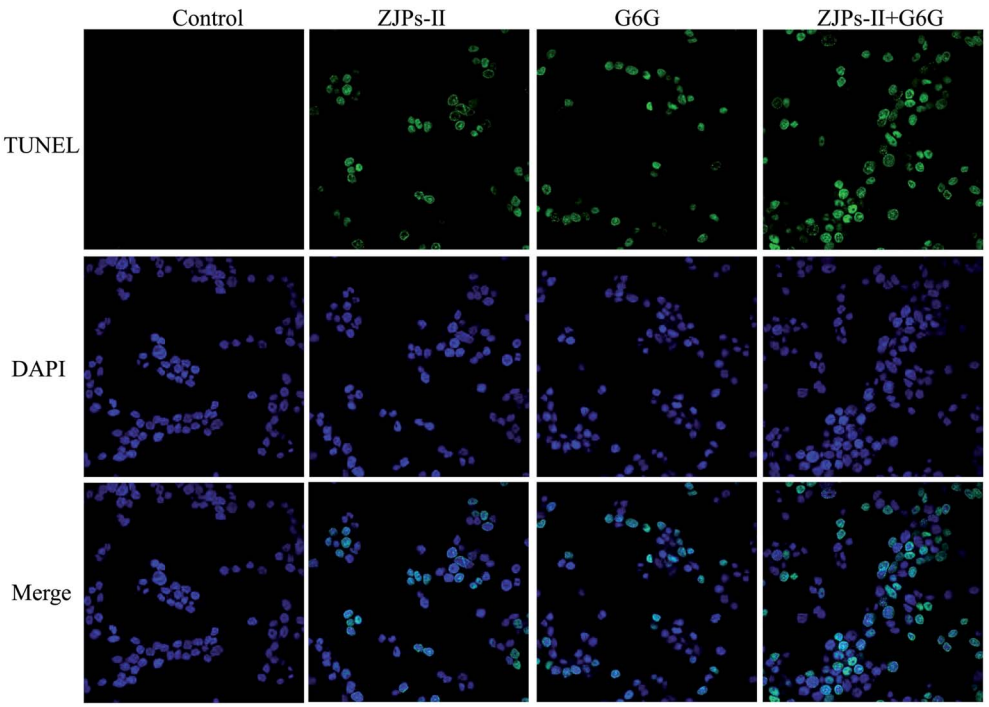

Fig. 7 Representative morphology of the SW620 cells under the control and incubated with IC_{50} concentrations of ZJPs-II and ginger 6-gingerol (G6G) alone and in combination for 24 h. SW620 cells were stained with TUNEL (green) and DAPI (blue). Fluorescence images were captured by confocal laser scanning microscopy (magnification, 600×).

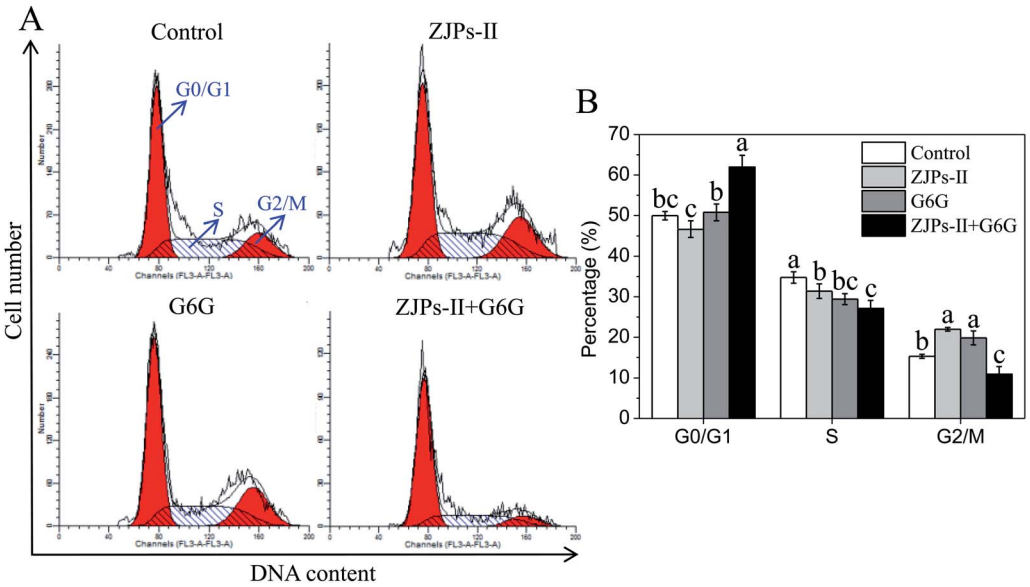

Fig. 8 Effects of ZJPs-II and ginger 6-gingerol (G6G) alone and in combination with IC_{50} concentrations on the cell-cycle phases (G0/G1, S, and G2/M) of SW620 cells. (A) Representative cytograms of the cell-cycle phases. Horizontal and vertical axes showed the relative nuclear DNA content and number of cells, respectively. (B) The cell population distribution in the different phases of the cell cycle. Data are expressed as the mean ± SD ($n = 3$). Different small letters represent the significant difference between the relative number of cells in each phase according to the LSD test ($p < 0.05$).

3.4.5. Discussion. Based on the practical experience of TCM and pharmacological studies, the joint effect of jujube and ginger might be due to the following three aspects: (i) harmonizing the nutrient *qi* and the defensive *qi via* balancing "*yin* and *yang*"; (ii) invigorating the spleen *qi* by jujube and reinforcing/protecting the stomach *qi* by ginger *via* remedying each other; and (iii) increasing therapeutic effects and attenuating toxicity and side-effect for many TCM decoctions (*e.g.*, Guizhi decoction, Xiaochaihu decoction).[64,65] More importantly, the decoctions from a combination of medicinal plants or herbs were commonly used in TCM, folk-medicine or herbal tea to maintain health and prevent/treat various diseases because of their synergistic effects.[66] The synergistic effects of various dietary compounds have been extensively found.[67] For example, Hu *et al.* found that the combination of *Chrysanthemum morifolum* and *Lycium barbarum* showed beneficial effects in diabetic rats, while *Chrysanthemum morifolum alone* did not exhibit protective effects.[68] Zhang *et al.* found that the synergistic antioxidant and anti-inflammatory mechanisms of the infusion of *Chrysanthemum* flower and wolfberry were due to their involved phenolics and polysaccharides through multiple inflammatory pathways.[69] In another example, Huang *et al.* found that the combination of Yupingfeng san (a representative formula in TCM) and *Flos Sophorae Immaturus* could be used to treat viral infections mainly due to the synergistic antioxidant activities of polysaccharides and total flavonoid for its clinical application.[70] They not only directly scavenge reactive oxygen species, but also indirectly protect the cell from oxidative damage. Recently, Li *et al.* reported that *Taraxacum officinale* root extract and *Radix Astragali* extract had synergistic hypoglycemic effect, which may be due to their rich in polysaccharides and phenolic compounds.[71] Therefore, the combinational use of natural herb products rich in polysaccharides and phenolic compounds is considered more effective on treatment of various diseases.

Previous studies have demonstrated that the antitumor mechanisms of polysaccharides include improving the immune response, preventing oncogenesis, inducing cancer cells apoptosis, regulating the apoptosis-related signaling pathway, inhibiting cancer cells progression, and/or prevention of their proliferation/migration.[52,55] As for 6-gingerol, its antitumor mechanism can be summarized as follows: (i) participating in enzymatic and/or non-enzymatic redox cycling and further causing the generation of reactive oxygen species in cancer cells and the decrease of the mitochondrial membrane potential;[29,72] (ii) inducing cellular damage and apoptosis;[29] and (iii) modulating tumor suppressor genes, cell-cycle, transcription factors, angiogenesis, and/or growth factors.[73] In terms of the present study, the simultaneous use of ZJPs-II and G6G could effectively prevent the growth of SW620 cells *via* inhibiting colony formation, inducing apoptosis and arresting the cell cycle at the G0/G1 stage. In consideration of the surmounting complexities of the signaling pathways by treating multiple therapeutic targets with the joint use of various natural compounds,[74] the corresponding inducing factors and mechanisms require further study. Moreover, this combined use might be related to their ability to exert synergistic effects *via* affecting complementary and susceptibility, and overlapping mechanisms of action because tumor cells are complex, diverse, and heterogeneous.[75] Despite the observed joint effects of ZJPs-II and G6G in our assay, identification of the exact effect mechanisms requires a further in-depth investigation from different

insights, such as the cell structure, gene regulation, expression pathways and other factors within cells *in vitro* and even *in vivo*. The addition of polyphenol might alter the topology conformation of polysaccharides chain *via* weak non-covalent interactions.[22] Zhu *et al.* probed the effects of the molecular structure of pectic polysaccharides and phenolic acids on their interactions, and found that the adsorption of phenolic acids by polysaccharides was due to their structures and driven by the hydrogen-bonding interactions.[76] By contrast, hydrophobic interactions might occur between the hydrophobic chains of polysaccharides and the aromatic rings of polyphenols.[77] The spontaneous adsorption of flavonoids by polysaccharides in corn silk was caused by hydrogen-bonding and van der Waals forces, and their interactions could enhance the α-amylase and α-glucosidase inhibitory activities of polysaccharides.[78] Accordingly, the hydrogen-bonding, hydrophobic and van der Waals forces had vital consequences on their physicochemical and nutritional properties of various foods and even medicines.[77,79]

Considering their structure determinants for bioactivity, further studies will be required to investigate the molecular interactions of jujube polysaccharides and ginger gingerols on their antioxidant and antitumor activities *via* changing the composition and M_w of ZJPs by jujube variety/extraction methods and gingerols/shogaols with different structure. Moreover, the interaction of ZJPs-II and G6G might change their absorption, distribution, metabolism processes, and even the gut microbiota in the gastrointestinal digestion when consumed orally in combination, which also required further studies. A previous study found that cell wall polysaccharide–polyphenol interactions reduced the polyphenol degradation during digestion, but favored the fermentation, beneficial gut microbiota and production of short-chain fatty acids.[77] As an example, Yang *et al.* found that cell wall polysaccharides modulated the polyphenol metabolites, short-chain fatty acid generation and probiotic growth, thus potentially enhancing the colonic health.[80] In another study, Bermúdez-Oria *et al.* reported that the pectin polysaccharides could maintain the antioxidant ability of 3,4-dihydroxyphenylglycol after digestion in the gastrointestinal tract, mainly due to the complexation and colon-targeted delivery effects.[81] Hu *et al.* reported that the combination of mulberry leaf and oat bran enriched in polyphenols and β-glucans could enhance the gut microbiota diversity and regulate their compositions.[82]

Nowadays, combined therapy possesses unique advantages compared to monotherapy, which may be due to their synergism, low side effects and dose-limiting toxicity.[83] Recently, Ye *et al.* found that the combination of *Lachnum* polysaccharide with silymarin could improve the antioxidant status, and protect acute liver injury by suppressing oxidative stress and inflammatory response.[84] Generally, both jujube and ginger were often used in the decoction and granule of TCM formulas and daily dietary therapy in China. Our data lay the theoretical foundation for the combined uptake of jujube and ginger. Our findings support the increasing and continuous consumption of jujube polysaccharides and gingerol in a combined strategy in our daily diet to achieve the equilibrium between "*yin* and *yang*" by the interaction among their nutritional and biological compounds. Therefore, on the one hand, the effect of the ratio of ZJPs-II and G6G on their bioactivities should be further investigated to achieve the optimal activity in combinatorial use. On the other hand, further efforts should be devoted to uncover the synergism and toxicity-reducing effects of the combinatorial use of jujube and ginger in the treatment of cancer *in vivo*.

4. Conclusions

In summary, we extracted and purified the main polysaccharide fraction from *Z. jujuba* as a potential anticancer compound, and further investigated the joint effects and preliminary working mechanisms of ZJPs-II and G6G alone and in combination on the antioxidant and antitumor activities. The obtained ZJPs-II with an average molecular-weight of 1.15×10^5 consisted of arabinose, rhamnose, glucose, xylose, and galactose. Their structural features were further analyzed by various instrumental characterizations. Results showed that ZJPs-II contained α- and β-glycosidic linkages, possessed high thermostability, and presented semi-crystalline morphology. ZJPs-II and G6G alone had obvious scavenging effects against DPPH˙ in a dose-dependent manner, and their combination presented the synergism effect at each dose. Furthermore, ZJPs-II and G6G alone dose-dependently inhibited the growth of SW620 cells with their IC_{50} of 752.3 and 66.0 μg mL^{-1} respectively, and their combination showed the synergistic effect at each dose. After treatment with IC_{50} concentrations of ZJPs-II and G6G alone and in combination, ZJPs-II and G6G alone showed strong inhibition in the proliferation and colony formation of SW620 cells *via* the apoptotic pathway and G2/M phase arrest of the cell cycle, while their combination exhibited higher inhibition activities on the proliferation and colony formation of SW620 cells *via* the apoptotic pathway and G0/G1 phase arrest mechanism. Using confocal laser scanning microscopy with TUNEL staining, the preliminary mechanism involved in the apoptosis and necrosis of SW620 cells treated by ZJPs-II and G6G alone and in combination was further verified morphologically. Taken together, this research suggests that ZJPs-II and G6G in combination can develop as an effective antitumor formulation for public health in functional foods and pharmaceuticals industries, which deserves further exploration. Our findings also recommend their combined intake in greater amounts in our daily diets for public health and preventing cancers.

Abbreviations

ZJPs	*Ziziphus jujuba* polysaccharides
ZJPs-II	The second main-fraction of ZJPs
G6G	Ginger 6-gingerol
DSC	Differential scanning calorimetry
TG	Thermogravimetric
DTG	The first derivative of thermogravimetric
XRD	X-ray diffraction
SEM	Scanning electron microscopy

AFM	Atomic force microscopy
DPPH$^{\cdot}$	1,1-Diphenyl-2-picrylhydrazyl free radical
CCK-8	Cell Counting Kit-8
DRI	Dose reduction index
CI	Combination index
TUNEL	TdT-mediated dUTP nick end labeling

Author contributions

Zhen Wu: conceptualization, data curation, investigation, methodology, validation, funding acquisition, project administration, supervision, visualization, writing – original draft, writing – review & editing. Ruiping Gao: investigation, methodology, validation. Hong Li: data curation, formal analysis, resources, writing – original draft, writing – review & editing. Yongde Wang: resources. Yang Luo: methodology. Jiang Zou: resources. Bo Zhao: writing – review & editing. Shiqi Chen: resources.

Conflicts of interest

All authors have no personal or financial conflicts of interest.

Acknowledgements

This work was supported by grants from the National Key R&D Program of China (No. 2017YFC1602000), Chongqing Science and Technology Bureau (No. cstc2019jxjl-jbky120003, cstc2019jcyj-msxmX0001, and cstc2019jscx-lyzxX0002), Chongqing Scientific Research Institutions Performance Incentive Guidance Project (No. jxjl20200004), Science and Technology Project of State Administration for Market Regulation of China (No. S2019MK463) and Young Talent Project of Chongqing Academy of Chinese Materia Medica (No. 2021-5).

References

1 State-Pharmacopoeia-Committee, *Pharmacopoeia of People's Republic of China (Part 1)*, China Medical Pharmaceutical Science and Technology Publishing House, Beijing, 2015, p. 22.
2 X. Shen, Y. Tang, R. Yang, L. Yu, T. Fang and J. A. Duan, The protective effect of *Zizyphus jujube* fruit on carbon tetrachloride-induced hepatic injury in mice by antioxidative activities, *J. Ethnopharmacol.*, 2009, **122**, 555–560.
3 J. Chen, M. Maiwulanjiang, K. Y. C. Lam, W. L. Zhang, J. Y. X. Zhan, C. T. W. Lam, S. L. Xu, K. Y. Zhu, P. Yao, D. T. W. Lau, T. T. X. Dong and K. W. K. Tsim, A standardized extract of the fruit of *Ziziphus jujuba* (jujube) induces neuronal differentiation of cultured PC12 Cells: a signaling mediated by protein kinase A, *J. Agric. Food Chem.*, 2014, **62**, 1890–1897.
4 Z. Rabiei, M. Rafieian-kopaei, E. Heidarian, E. Saghaei and S. Mokhtari, Effects of *Zizyphus jujube* extract on memory and learning impairment induced by bilateral electric lesions of the nucleus basalis of meynert in rat, *Neurochem. Res.*, 2014, **39**, 353–360.
5 D. Cheng, C. Zhu, J. Cao and W. Jiang, The protective effects of polyphenols from jujube peel (*Ziziphus Jujube* Mill) on isoproterenol-induced myocardial ischemia and aluminum-induced oxidative damage in rats, *Food Chem. Toxicol.*, 2012, **50**, 1302–1308.
6 J. Reche, F. Hernández, M. S. Almansa, Á. A. Carbonell-Barrachina, P. Legua and A. Amorós, Physicochemical and nutritional composition, volatile profile and antioxidant activity differences in Spanish jujube fruits, *LWT–Food Sci. Technol.*, 2018, **98**, 1–8.
7 J. Reche, F. Hernández, M. S. Almansa, Á. A. Carbonell-Barrachina, P. Legua and A. Amorós, Effects of organic and conventional farming on the physicochemical and functional properties of jujube fruit, *LWT–Food Sci. Technol.*, 2019, **99**, 438–444.
8 Y. Wang, Y. Xu, X. Ma, X. Liu, M. Yang, W. Fan, H. Ren, N. Efehi, X. Wang and X. Zhu, Extraction, purification, characterization and antioxidant activities of polysaccharides from *Zizyphus jujuba cv. Linzexiaozao*, *Int. J. Biol. Macromol.*, 2018, **118**, 2138–2148.
9 S. Sang, H. D. Snook, F. S. Tareq and Y. Fasina, Precision research on ginger: the type of ginger matters, *J. Agric. Food Chem.*, 2020, **68**, 8517–8523.
10 B. H. Ali, G. Blunden, M. O. Tanira and A. Nemmar, Some phytochemical, pharmacological and toxicological properties of ginger (*Zingiber officinale* Roscoe): A review of recent research, *Food Chem. Toxicol.*, 2008, **46**, 409–420.
11 A. M. Al Hroob, M. H. Abukhalil, R. D. Alghonmeen and A. M. Mahmoud, Ginger alleviates hyperglycemia-induced oxidative stress, inflammation and apoptosis and protects rats against diabetic nephropathy, *Biomed. Pharmacother.*, 2018, **106**, 381–389.
12 M. J. Ko, H. H. Nam and M. S. Chung, Conversion of 6-gingerol to 6-shogaol in ginger (*Zingiber officinale*) pulp and peel during subcritical water extraction, *Food Chem.*, 2019, **270**, 149–155.
13 S. Z. Jiang, N. S. Wang and S. Q. Mi, Plasma pharmacokinetics and tissue distribution of [6]-gingerol in rats, *Biopharm. Drug Dispos.*, 2008, **29**, 529–537.
14 J. Yamahara, Q. R. Huang, Y. H. Li, L. Xu and H. Fujimura, Gastrointestinal motility enhancing effect of ginger and its active constituents, *Chem. Pharm. Bull.*, 1990, **38**, 430–431.
15 Y. Zhang, H. Li, M. Huang, K. Chu, W. Xu, S. Zhang, J. Que and L. Chen, Neuroprotective effects of Gualou Guizhi decoction *in vivo* and *in vitro*, *J. Ethnopharmacol.*, 2014, **158**, 76–84.
16 R. Wang, Y. Peng, H. Meng and X. Li, Protective effect of polysaccharides fractions from Sijunzi decoction in reserpine-induced spleen deficiency rats, *RSC Adv.*, 2016, **6**, 60657–60665.
17 X. Huang, A. Kojima-Yuasa, S. Xu, D. O. Kennedy, T. Hasuma and I. Matsui-Yuasa, Combination of *Zizyphus jujuba* and green tea extracts exerts excellent cytotoxic activity in HepG2 cells *via* reducing the expression of APRIL, *Am. J. Chin. Med.*, 2009, **37**, 169–179.
18 X. Fang, Y. Jiang, H. Ji, L. Zhao, W. Xiao, Z. Wang and G. Ding, The synergistic beneficial effects of ginkgo

flavonoid and *Coriolus versicolor* polysaccharide for memory improvements in a mouse model of dementia, *J. Evidence-Based Complementary Altern. Med.*, 2015, **2015**, 128394.

19 S. Khawas, G. Nosáľová, S. K. Majee, K. Ghosh, W. Raja, V. Sivová and B. Ray, *In vivo* cough suppressive activity of pectic polysaccharide with arabinogalactan type II side chains of *Piper nigrum* fruits and its synergistic effect with piperine, *Int. J. Biol. Macromol.*, 2017, **99**, 335–342.

20 J. Wang, W. Liu, Z. Chen and H. Chen, Physicochemical characterization of the oolong tea polysaccharides with high molecular weight and their synergistic effects in combination with polyphenols on hepatocellular carcinoma, *Biomed. Pharmacother.*, 2017, **90**, 160–170.

21 J. Li, R. Li, N. Li, F. Zheng, Y. Dai, Y. Ge, H. Yue and S. Yu, Mechanism of antidiabetic and synergistic effects of ginseng polysaccharide and ginsenoside Rb1 on diabetic rat model, *J. Pharm. Biomed. Anal.*, 2018, **158**, 451–460.

22 J. You, Y. Chang, D. Zhao, J. Zhuang and W. Zhuang, A mixture of functional complex extracts from *Lycium barbarum* and grape seed enhances immunity synergistically *in vitro* and *in vivo*, *J. Food Sci.*, 2019, **84**, 1577–1585.

23 X. Chen, L. Qian, B. Wang, Z. Zhang, H. Liu, Y. Zhang and J. Liu, Synergistic hypoglycemic effects of pumpkin polysaccharides and puerarin on type II diabetes mellitus mice, *Molecules*, 2019, **24**, 955.

24 J. Liu, R. Bai, Y. Liu, X. Zhang, J. Kan and C. Jin, Isolation, structural characterization and bioactivities of naturally occurring polysaccharide–polyphenolic conjugates from medicinal plants—A reivew, *Int. J. Biol. Macromol.*, 2018, **107**, 2242–2250.

25 Y. Fan, Y. Hu, D. Wang, Z. Guo, X. Zhao, L. Guo, B. Zhao, J. Zhang, Y. Wang and T. L. Nguyen, Epimedium polysaccharide and propolis flavone can synergistically stimulate lymphocyte proliferation *in vitro* and enhance the immune responses to ND vaccine in chickens, *Int. J. Biol. Macromol.*, 2010, **47**, 87–92.

26 D. Tang, S. Zhang, X. Shi, J. Wu, G. Yin, X. Tan, F. Liu, X. Wu and X. Du, Combination of *astragali* polysaccharide and curcumin improves the morphological structure of tumor vessels and induces tumor vascular normalization to inhibit the growth of hepatocellular carcinoma, *Integr. Cancer Ther.*, 2019, **18**, 1–8.

27 Y. Wang, X. Liu, J. Zhang, G. Liu, Y. Liu, K. Wang, M. Yang, H. Cheng and Z. Zhao, Structural characterization and *in vitro* antitumor activity of polysaccharides from *Zizyphus jujuba cv. Muzao*, *RSC Adv.*, 2015, **5**, 7860–7867.

28 X. Ji, C. Hou, X. Zhang, L. Han, S. Yin, Q. Peng and M. Wang, Microbiome-metabolomic analysis of the impact of *Zizyphus jujuba cv. Muzao* polysaccharides consumption on colorectal cancer mice fecal microbiota and metabolites, *Int. J. Biol. Macromol.*, 2019, **131**, 1067–1076.

29 R. M. T. de Lima, A. C. dos Reis, J. V. de Oliveira Santos, J. R. de Oliveira Ferreira, A. Lima Braga, J. W. G. de Oliveira Filho, A. A. P. M. de Menezes, A. M. O. F. da Mata, M. V. O. B. de Alencar, D. C. do Nascimento Rodrigues, P. M. Pinheiro Ferreira, T. de Jesus Aguiar dos Santos Andrade, J. C. Ramos Gonçalves, F. C. Carneiro da Silva, J. M. de Castro e Sousa and A. A. de Carvalho Melo Cavalcante, Toxic, cytogenetic and antitumor evaluations of [6]-gingerol in non-clinical *in vitro* studies, *Biomed. Pharmacother.*, 2019, **115**, 108873.

30 Z. Wu, H. Li, Y. Wang, D. Yang, H. Tan, Y. Zhan, Y. Yang, Y. Luo and G. Chen, Optimization extraction, structural features and antitumor activity of polysaccharides from *Z. jujuba cv. Ruoqiangzao* seeds, *Int. J. Biol. Macromol.*, 2019, **135**, 1151–1161.

31 M. DuBois, K. A. Gilles, J. K. Hamilton, P. A. Rebers and F. Smith, Colorimetric method for determination of sugars and related substances, *Anal. Chem.*, 1956, **28**, 350–356.

32 AOAC, Association of Official Analytical Chemists, *Official methods of analysis*, USA, Washington, DC, 15th edn, 1990.

33 N. Blumenkrantz and G. Asboe-Hansen, New method for quantitative determination of uronic acids, *Anal. Biochem.*, 1973, **54**, 484–489.

34 Z. Wu, Effect of different drying methods on chemical composition and bioactivity of finger citron polysaccharides, *Int. J. Biol. Macromol.*, 2015, **76**, 218–223.

35 C. Kuei-Ting, Drug combination studies and their synergy quantification using the Chou-Talalay, *Cancer Res.*, 2010, **70**, 440–446.

36 G. Sharmila, C. Muthukumaran, E. Suriya, R. Muppidathi Keerthana, M. Kamatchi, N. M. Kumar, T. Anbarasan and J. Jeyanthi, Ultrasound aided extraction of yellow pigment from *Tecoma castanifolia* floral petals: Optimization by response surface method and evaluation of the antioxidant activity, *Ind. Crops Prod.*, 2019, **130**, 467–477.

37 Y. Wang, N. Liu, X. Xue, Q. Li, D. Sun and Z. Zhao, Purification, structural characterization and *in vivo* immunoregulatory activity of a novel polysaccharide from *Polygonatum sibiricum*, *Int. J. Biol. Macromol.*, 2020, **160**, 688–694.

38 Y. Y. Ren, Z. Y. Zhu, H. Q. Sun and L. J. Chen, Structural characterization and inhibition on α-glucosidase activity of acidic polysaccharide from *Annona squamosa*, *Carbohydr. Polym.*, 2017, **174**, 1–12.

39 W. Chen, Z. Jia, J. Zhu, Y. Zou, G. Huang and Y. Hong, Optimization of ultrasonic-assisted enzymatic extraction of polysaccharides from thick-shell mussel (*Mytilus coruscus*) and their antioxidant activities, *Int. J. Biol. Macromol.*, 2019, **140**, 1116–1125.

40 X. Gao, H. Qu, S. Shan, C. Song, D. Baranenko, Y. Li and W. Lu, A novel polysaccharide isolated from *Ulva pertusa*: Structure and physicochemical property, *Carbohydr. Polym.*, 2020, **233**, 115849.

41 H. Li, Y. Mi, Z. Duan, P. Ma and D. Fan, Structural characterization and immunomodulatory activity of a polysaccharide from *Eurotium cristatum*, *Int. J. Biol. Macromol.*, 2020, **162**, 609–617.

42 Y. Bai, X. Jia, F. Huang, R. Zhang, L. Dong, L. Liu and M. Zhang, Structural elucidation, anti-inflammatory activity and intestinal barrier protection of longan pulp polysaccharide LPIIa, *Carbohydr. Polym.*, 2020, **246**, 116532.

43 R. Sorourian, A. E. Khajehrahimi, M. Tadayoni, M. H. Azizi and M. Hojjati, Ultrasound-assisted extraction of polysaccharides from *Typha domingensis*: Structural characterization and functional properties, *Int. J. Biol. Macromol.*, 2020, **160**, 758–768.

44 G. Chen, C. Fang, X. Chen, Z. Wang, M. Liu and J. Kan, High-pressure ultrasonic-assisted extraction of polysaccharides from *Mentha haplocalyx*: Structure, functional and biological activities, *Ind. Crops Prod.*, 2019, **130**, 273–284.

45 X. Ji, F. Zhang, R. Zhang, F. Liu, Q. Peng and M. Wang, An acidic polysaccharide from *Ziziphus Jujuba cv. Muzao*: Purification and structural characterization, *Food Chem.*, 2019, **274**, 494–499.

46 X. Ji, C. Hou, Y. Yan, M. Shi and Y. Liu, Comparison of structural characterization and antioxidant activity of polysaccharides from jujube (*Ziziphus jujuba* Mill.) fruit, *Int. J. Biol. Macromol.*, 2020, **149**, 1008–1018.

47 Y. Wang, X. Zhang, X. Ma, K. Zhang, S. Li, X. Wang, X. Liu, J. Liu, W. Fan, Y. Li, Q. Li and X. Zhu, Study on the kinetic model, thermodynamic and physicochemical properties of *Glycyrrhiza* polysaccharide by ultrasonic assisted extraction, *Ultrason. Sonochem.*, 2019, **51**, 249–257.

48 F. Chemat, N. Rombaut, A. G. Sicaire, A. Meullemiestre, A. S. Fabiano-Tixier and M. Abert-Vian, Ultrasound assisted extraction of food and natural products. Mechanisms, techniques, combinations, protocols and applications. A review, *Ultrason. Sonochem.*, 2017, **34**, 540–560.

49 E. I. Nep and B. R. Conway, Physicochemical characterization of grewia polysaccharide gum: Effect of drying method, *Carbohydr. Polym.*, 2011, **84**, 446–453.

50 J. K. Yan, Y. Y. Wang, W. Y. Qiu, Z. B. Wang and H. Ma, Ultrasound synergized with three-phase partitioning for extraction and separation of *Corbicula fluminea* polysaccharides and possible relevant mechanisms, *Ultrason. Sonochem.*, 2018, **40**, 128–134.

51 M. Anwar, M. McConnell and A. E. D. Bekhit, New freeze-thaw method for improved extraction of water-soluble non-starch polysaccharide from taro (*Colocasia esculenta*): Optimization and comprehensive characterization of physico-chemical and structural properties, *Food Chem.*, 2021, **349**, 129210.

52 X. Ji, Q. Peng, Y. Yuan, J. Shen, X. Xie and M. Wang, Isolation, structures and bioactivities of the polysaccharides from jujube fruit (*Ziziphus jujuba* Mill.): A review, *Food Chem.*, 2017, **227**, 349–357.

53 L. Tabrizi, D. Q. Dao and T. A. Vu, Experimental and theoretical evaluation on the antioxidant activity of a copper(ii) complex based on lidocaine and ibuprofen amide-phenanthroline agents, *RSC Adv.*, 2019, **9**, 3320–3335.

54 S. Afrin, F. Giampieri, T. Y. Forbes-Hernández, M. Gasparrini, A. Amici, D. Cianciosi, J. L. Quiles and M. Battino, Manuka honey synergistically enhances the chemopreventive effect of 5-fluorouracil on human colon cancer cells by inducing oxidative stress and apoptosis, altering metabolic phenotypes and suppressing metastasis ability, *Free Radical Biol. Med.*, 2018, **126**, 41–54.

55 X. Wang, A. Gao, Y. Jiao, Y. Zhao and X. Yang, Antitumor effect and molecular mechanism of antioxidant polysaccharides from *Salvia miltiorrhiza* Bunge in human colorectal carcinoma LoVo cells, *Int. J. Biol. Macromol.*, 2018, **108**, 625–634.

56 Z. J. Wang, J. H. Xie, S. P. Nie and M. Y. Xie, Review on cell models to evaluate the potential antioxidant activity of polysaccharides, *Food Funct.*, 2017, **8**, 915–926.

57 H. Bai, Z. Wang, J. Cui, K. Yun, H. Zhang, R. H. Liu, Z. Fan and C. Cheng, Synergistic radiation protective effect of purified *auricularia auricular-judae* polysaccharide (AAP IV) with grape seed procyanidins, *Molecules*, 2014, **19**, 20675–20694.

58 D. Ren, Y. Jiao, X. Yang, L. Yuan, J. Guo and Y. Zhao, Antioxidant and antitumor effects of polysaccharides from the fungus *Pleurotus abalonus*, *Chem.-Biol. Interact.*, 2015, **237**, 166–174.

59 Z. Wu, H. Li, Y. Luo, G. Chen, J. Li, Y. Wang, Y. Yang and H. Tan, Insights into the structural characterisations, bioactivities and their correlations with water-soluble polysaccharides extracted from different pomelo (*Citrus maxima* Merr.) tissues, *Int. J. Food Sci. Technol.*, 2020, **55**, 3091–3103.

60 L. C. G. F. Palhares, J. S. Barbosa, K. C. Scortecci, H. A. O. Rocha, A. S. Brito and S. F. Chavante, *In vitro* antitumor and anti-angiogenic activities of a shrimp chondroitin sulfate, *Int. J. Biol. Macromol.*, 2020, **162**, 1153–1165.

61 N. Aceto, A. Bardia, D. T. Miyamoto, M. C. Donaldson, B. S. Wittner, J. A. Spencer, M. Yu, A. Pely, A. Engstrom, H. Zhu, B. W. Brannigan, R. Kapur, S. L. Stott, T. Shioda, S. Ramaswamy, D. T. Ting, C. P. Lin, M. Toner, D. A. Haber and S. Maheswaran, Circulating tumor cell clusters are oligoclonal precursors of breast cancer metastasis, *Cell*, 2014, **158**, 1110–1122.

62 Q. Huang, L. Zhang, P. C. K. Cheung and X. Tan, Evaluation of sulfated α-glucans from *Poria cocos* mycelia as potential antitumor agent, *Carbohydr. Polym.*, 2006, **64**, 337–344.

63 L. Papucci, L. Formigli, N. Schiavone, A. Tani, M. Donnini, A. Lapucci, F. Perna, A. Tempestini, E. Witort, M. Morganti, D. Nosi, G. E. Orlandini, S. Zecchi Orlandini and S. Capaccioli, Apoptosis shifts to necrosis *via* intermediate types of cell death by a mechanism depending on *c-myc* and *bcl-2* expression, *Cell Tissue Res.*, 2004, **316**, 197–209.

64 C. T. W. Lam, P. H. Chan, P. S. C. Lee, K. M. Lau, A. Y. Y. Kong, A. G. W. Gong, M. L. Xu, K. Y. C. Lam, T. T. X. Dong, H. Lin and K. W. K. Tsim, Chemical and biological assessment of Jujube (*Ziziphus jujuba*)-containing herbal decoctions: Induction of erythropoietin expression in cultures, *J. Chromatogr. B: Anal. Technol. Biomed. Life Sci.*, 2016, **1026**, 254–262.

65 C. T. W. Lam, A. G. W. Gong, K. Y. C. Lam, L. M. Zhang, J. P. Chen, T. T. X. Dong, H. Q. Lin and K. W. K. Tsim, Jujube-containing herbal decoctions induce neuronal differentiation and the expression of anti-oxidant enzymes

in cultured PC12 cells, *J. Ethnopharmacol.*, 2016, **188**, 275–283.

66 I. J. Atangwho, P. E. Ebong, E. U. Eyong, M. Z. Asmawi and M. Ahmad, Synergistic antidiabetic activity of *Vernonia amygdalina* and *Azadirachta indica*: Biochemical effects and possible mechanism, *J. Ethnopharmacol.*, 2012, **141**, 878–887.

67 T. M. de Kok, S. G. van Breda and M. M. Manson, Mechanisms of combined action of different chemopreventive dietary compounds, *Eur. J. Nutr.*, 2008, **47**, 51–59.

68 C. K. Hu, Y. J. Lee, C. M. Colitz, C. J. Chang and C. T. Lin, The protective effects of *Lycium barbarum* and *Chrysanthemum morifolum* on diabetic retinopathies in rats, *Vet. Ophthalmol.*, 2012, **15**, 65–71.

69 N. Zhang, Z. He, S. He and P. Jing, Insights into the importance of dietary chrysanthemum flower (*Chrysanthemum morifolium* cv. Hangju)-wolfberry (*Lycium barbarum* fruit) combination in antioxidant and anti-inflammatory properties, *Food Res. Int.*, 2019, **116**, 810–818.

70 R. Huang, Y. Zhang, Y. Zhang, L. Zhang, L. Pei, G. Shu, Z. Yuan, J. Lin, G. Peng, W. Zhang, L. Zhao, F. Shi and H. Fu, Evaluation of the synergetic effect of Yupingfeng san and *Flos Sophorae Immaturus* based on free radical scavenging capacity, *Biomed. Pharmacother.*, 2020, **128**, 110265.

71 J. Li, J. Luo, Y. Chai, Y. Guo, Y. Tianzhi and Y. Bao, Hypoglycemic effect of *Taraxacum officinale* root extract and its synergism with *Radix Astragali* extract, *Food Sci. Nutr.*, 2021, **9**, 2075–2085.

72 D. P. Mansingh, S. O. J, V. K. Sali and H. R. Vasanthi, [6]-Gingerol-induced cell cycle arrest, reactive oxygen species generation, and disruption of mitochondrial membrane potential are associated with apoptosis in human gastric cancer (AGS) cells, *J. Biochem. Mol. Toxicol.*, 2018, **32**, e22206.

73 A. Ahmad, A. A. Mohammed, A. Faris, S. A. Khaled and H. R. Arshad, Ginger: a novel strategy to battle cancer through modulating cell signalling pathways: A review, *Curr. Pharm. Biotechnol.*, 2019, **20**, 5–16.

74 S. Liu, R. Li, J. Qian, J. Sun, G. Li, J. Shen and Y. Xie, Combination therapy of doxorubicin and quercetin on multidrug-resistant breast cancer and their sequential delivery by reduction-sensitive hyaluronic acid-based conjugate/D-α-tocopheryl poly(ethylene glycol) 1000 succinate mixed micelles, *Mol. Pharm.*, 2020, **17**, 1415–1427.

75 R. H. Liu, Potential synergy of phytochemicals in cancer prevention: Mechanism of action, *J. Nutr.*, 2004, **134**, 3479S–3485S.

76 J. Zhu, D. Zhang, H. Tang and G. Zhao, Structure relationship of non-covalent interactions between phenolic acids and arabinan-rich pectic polysaccharides from rapeseed meal, *Int. J. Biol. Macromol.*, 2018, **120**, 2597–2603.

77 X. Liu, C. Le Bourvellec and C. M. G. C. Renard, Interactions between cell wall polysaccharides and polyphenols: Effect of molecular internal structure, *Compr. Rev. Food Sci. Food Saf.*, 2020, **19**, 3574–3617.

78 Q. Guo, Q. Ma, Z. Xue, X. Gao and H. Chen, Studies on the binding characteristics of three polysaccharides with different molecular weight and flavonoids from corn silk (*Maydis stigma*), *Carbohydr. Polym.*, 2018, **198**, 581–588.

79 F. Zhu, Interactions between cell wall polysaccharides and polyphenols, *Crit. Rev. Food Sci. Nutr.*, 2018, **58**, 1808–1831.

80 Z. Yang, T. Huang, P. Li, J. Ai, J. Liu, W. Bai and L. Tian, Dietary fiber modulates the fermentation patterns of cyanidin-3-O-glucoside in a fiber-type dependent manner, *Foods*, 2021, **10**, 1386.

81 A. Bermúdez-Oria, G. Rodríguez-Gutiérrez, E. Rodríguez-Juan, A. González-Benjumea and J. Fernández-Bolaños, Molecular interactions between 3,4-dihydroxyphenylglycol and pectin and antioxidant capacity of this complex *in vitro*, *Carbohydr. Polym.*, 2018, **197**, 260–268.

82 T. G. Hu, P. Wen, J. Liu, X. S. Long, S. T. Liao, H. Wu and Y. X. Zou, Combination of mulberry leaf and oat bran possessed greater hypoglycemic effect on diabetic mice than mulberry leaf or oat bran alone, *J. Funct. Foods*, 2019, **61**, 103503.

83 A. Ediriwickrema and W. M. Saltzman, Nanotherapy for cancer: targeting and multifunctionality in the future of cancer therapies, *ACS Biomater. Sci. Eng.*, 2015, **1**, 64–78.

84 Z. Ye, X. Zhang, Q. Huang, W. Zhang and M. Ye, Synergistic hepatoprotective effect of combined administration of *Lachnum* polysaccharide with silymarin, *Bioorg. Med. Chem. Lett.*, 2021, **46**, 128159.